



Identifying *Isl1* Genetic Lineage in the Developing Olfactory System and in GnRH-1 Neurons

Ed Zandro M. Taroc, Raghu Ram Katreddi and Paolo E. Forni*

Department of Biological Sciences, The RNA Institute, and the Center for Neuroscience Research, University at Albany, State University of New York, Albany, NY, United States

OPEN ACCESS

Edited by:

Lisa Taneyhill,
University of Maryland, College Park,
United States

Reviewed by:

Anna Cariboni,
University of Milan, Italy
Vincent Prevot,
Institut National de la Santé et de la
Recherche Médicale (INSERM),
France

*Correspondence:

Paolo E. Forni
pforni@albany.edu

Specialty section:

This article was submitted to
Craniofacial Biology and Dental
Research,
a section of the journal
Frontiers in Physiology

Received: 02 September 2020

Accepted: 30 September 2020

Published: 21 October 2020

Citation:

Taroc EZM, Katreddi RR and
Forni PE (2020) Identifying *Isl1*
Genetic Lineage in the Developing
Olfactory System and in GnRH-1
Neurons. *Front. Physiol.* 11:601923.
doi: 10.3389/fphys.2020.601923

During embryonic development, symmetric ectodermal thickenings [olfactory placodes (OP)] give rise to several cell types that comprise the olfactory system, such as those that form the terminal nerve ganglion (TN), gonadotropin releasing hormone-1 neurons (GnRH-1ns), and other migratory neurons in rodents. Even though the genetic heterogeneity among these cell types is documented, unidentified cell populations arising from the OP remain. One candidate to identify placodal derived neurons in the developing nasal area is the transcription factor *Isl1*, which was recently identified in GnRH-3 neurons of the terminal nerve in fish, as well as expression in neurons of the nasal migratory mass (MM). Here, we analyzed the *Isl1* genetic lineage in chemosensory neuronal populations in the nasal area and migratory GnRH-1ns in mice using *in situ* hybridization, immunolabeling a Tamoxifen inducible *Isl1*Cre^{ERT} and a constitutive *Isl1*^{Cre} knock-in mouse lines. In addition, we also performed conditional *Isl1* ablation in developing GnRH neurons. We found *Isl1* lineage across non-sensory cells of the respiratory epithelium and sustentacular cells of OE and VNO. We identified a population of transient embryonic *Isl1* + neurons in the olfactory epithelium and sparse *Isl1* + neurons in postnatal VNO. *Isl1* is expressed in almost all GnRH neurons and in approximately half of the other neuron populations in the MM. However, *Isl1* conditional ablation alone does not significantly compromise GnRH-1 neuronal migration or GnRH-1 expression, suggesting compensatory mechanisms. Further studies will elucidate the functional and mechanistic role of *Isl1* in development of migratory endocrine neurons.

Keywords: olfactory neurons, vomeronasal sensory neurons, GnRH neurons, *Isl1*, *Isl1* conditional knock-out, genetic lineage tracing, olfactory placode, neural crest

INTRODUCTION

Cranial placodes are specialized regions of ectoderm, that give rise to the pituitary gland, sensory organs, and ganglia of the vertebrate head (Brugmann and Moody, 2005; Schlosser, 2006). They form as a result of specific expression patterns of transcription factors in pre-placodal ectoderm surrounding the anterior neural plate (Brugmann and Moody, 2005; Bailey and Streit, 2006). In mice, the olfactory placodes (OPs) are morphologically identifiable at embryonic day 9.5 (E9.5), as a bilateral ectoderm thickening in the antero-lateral region of the head (**Figure 1**). The transcription

factors Oct1, Sox2, Pou2f1, Pax6, Eya1, Six1, Six4, Ngn1, Hes1, Hes5, MASH1/Ascl1, Ngn1, and Gli3 have been identified to control various steps of OP induction/formation, neurogenesis, neuronal development, and expression of olfactory specific genes (Cau et al., 1997, 2002; Zou et al., 2004; Donner et al., 2007; Schlosser et al., 2008; Chen et al., 2009; Riddiford and Schlosser, 2016).

The olfactory pit of vertebrates generates neurogenic and non-neurogenic progenitors. The non-neurogenic portions of the olfactory pit give rise to the respiratory epithelium, which is located in the rostral olfactory pit, while the neurogenic portions give rise to specific neuronal and glial/support cells (Figures 1, 2). The respiratory epithelium, which is the main source of Fgf8, controls the development of the neural crest derived nasal mesenchyme and bones (Forni et al., 2013). Neurogenic waves in the olfactory pit of mice first gives rise to mostly migratory neurons (Fornaro et al., 2003; Forni et al., 2013) such as early pioneer olfactory neurons, neurons of the terminal nerve, including Gonadotropin releasing hormone-1 neurons (GnRH-1ns), NPY positive migratory neurons, and other neurons with unknown identity and function or neurons of the migratory mass (MM) (Schwanzel-Fukuda and Pfaff, 1989; Wray et al., 1989; Hilal et al., 1996; Fornaro et al., 2007). The nasal area of mice contains several other neuronal cell types that include specialized olfactory sensory neurons (OSNs) such as the guanylyl cyclase-D (GC-D) neurons of the necklace olfactory system (Luo, 2008; Mori et al., 2014; Greer et al., 2016), microvillar cells (MVCs) (Pfister et al., 2012), sensory neurons of the septal organ (SO) (Ma et al., 2003), the Grueneberg ganglion (GG) (Gruneberg, 1973; Schmid et al., 2010; Mamasuew et al., 2011; Matsuo et al., 2012; Moine et al., 2018), and cells forming the terminal nerve ganglion (TN) (Larsell, 1950; Brown, 1987; Jennes, 1987; Oelschlager et al., 1987; Schwanzel-Fukuda et al., 1987; Wirsig-Wiechmann, 2004; Taroc et al., 2017; Jin et al., 2019) including the GnRH-1ns (Schwanzel-Fukuda and Pfaff, 1989; Wray et al., 1989). The mechanisms and molecules that drive progenitors of the developing olfactory pit into early migratory cells types remain largely unknown.

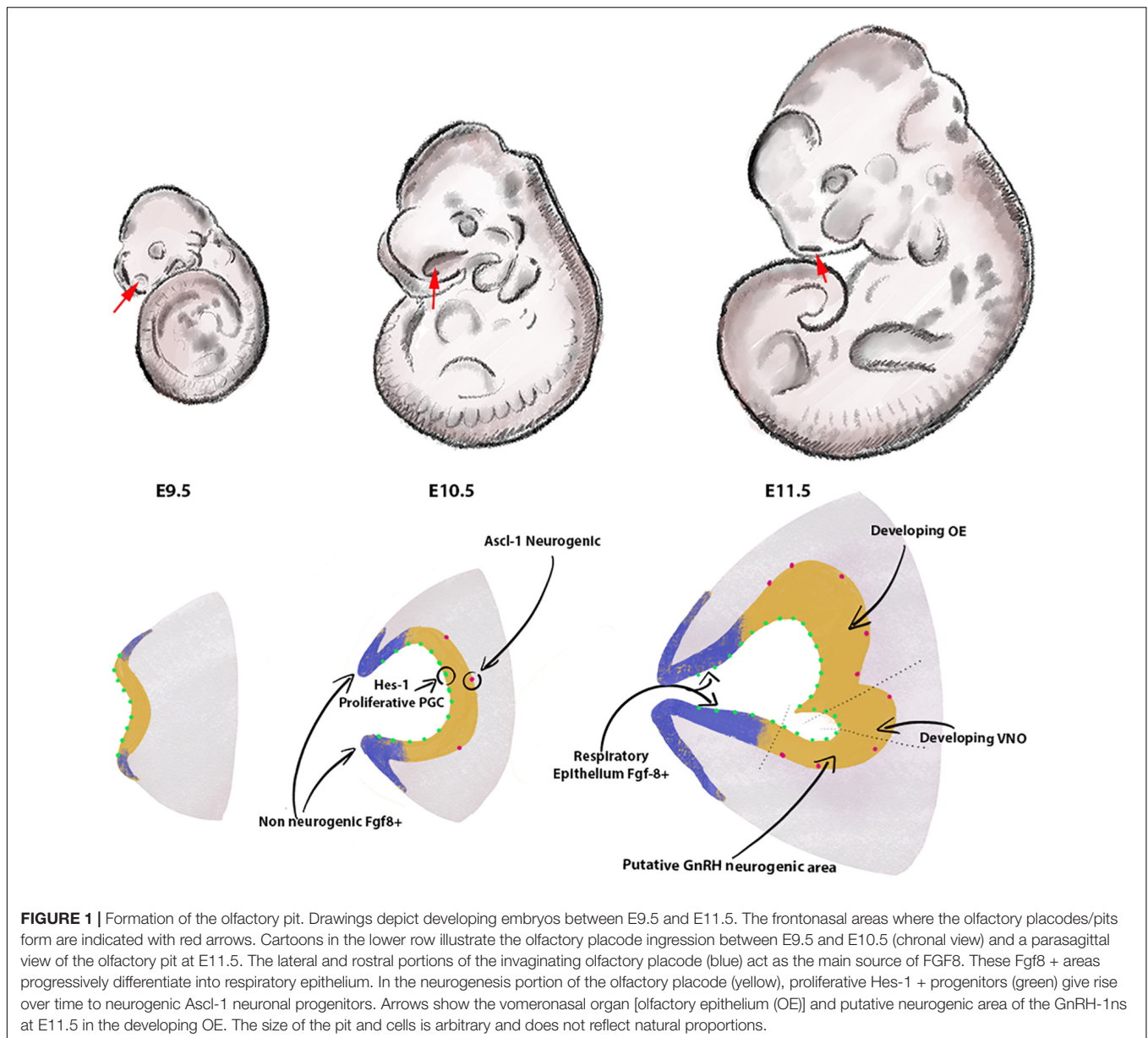
Between E9.5 and E10.5, the OPs begin to ingress to form the olfactory pits that give rise to various cellular components of the nose during development (Cuschieri and Bannister, 1975b; Chen et al., 2009). The olfactory pit is largely populated by proliferative progenitors expressing the transcription factors Hes1 + /Hes5. These early progenitors undergo mitosis in the apical portion of the epithelium and give rise over time to neurogenic progenitors positive for the bHLH transcription factor Ascl-1 (Cuschieri and Bannister, 1975a,b; Cau et al., 2000; Taroc et al., 2020). Gli3 influences proliferative Hes1 + positive progenitors to give rise to Ascl-1 + neurogenic progenitors that eventually generate OSNs and vomeronasal sensory neurons (VSNs) (Cau et al., 2000; Taroc et al., 2020). Notably, Gli3 loss of function does not prevent neurogenesis of GnRH-1ns, suggesting that these have a distinct lineage from the olfactory neurons.

GnRH-1ns are the initial neuronal population to form in the developing olfactory pit (Wray et al., 1989; Fornaro

et al., 2003). During embryonic development, GnRH-1ns migrate along the axons of the terminal nerve (Taroc et al., 2017) from the nasal area to the basal forebrain. Once in brain the GnRH-1ns control the release of gonadotropins from the pituitary gland (Forni and Wray, 2015). Aberrant development or function of GnRH-1ns causes hypogonadotropic hypogonadism (HH) (Cattanach et al., 1977), that can lead to a spectrum of reproductive disorders (Balasubramanian et al., 2010). GnRH-1 neuronal migration strictly depends on correct development and maturation of the neural crest derived olfactory ensheathing cells (Barraud et al., 2013; Pingault et al., 2013; Zhou et al., 2017; Wang et al., 2018). Cre genetic lineage tracing and BAC transgenic reporters have revealed extensive genetic heterogeneity among neurons that originate in the olfactory area of mice including the GnRH-1ns, suggesting a potential integration of neural crest cells in the developing OP (Forni et al., 2011b; Katoh et al., 2011; Suzuki and Osumi, 2015; Taroc et al., 2017; Shan et al., 2020). However, the mechanisms that give rise to the GnRH neurons and the required transcription factors for these regulatory processes remain unresolved.

The LIM-homeodomain transcription factor Isl1 has been recently identified in subsets of neuronal derivatives forming from the OP (Aguillon et al., 2018; Palaniappan et al., 2019; Shan et al., 2020). Isl1/2 expression occurs in GnRH expressing neurons and other putative neurons of the terminal nerve (Aguillon et al., 2018; Palaniappan et al., 2019; Lund et al., 2020; Shan et al., 2020) in chick, zebrafish, mouse, and humans. In zebrafish (Aguillon et al., 2018), Isl1/2 is expressed in terminal nerve GnRH-3 neurons associated with the olfactory epithelium. These neuro-modulatory cells, which are non-migratory in fish, exert the same physiological function as migratory GnRH-1ns in mice (Forni and Wray, 2015). The terminal nerve and MM in birds contains heterogeneous populations of (1) cells that express GnRH-1 but are negative for Isl1/2 and Lhx2, (2) cells only expressing Lhx2, (3) cells only positive for Isl1, and (4) cells that co-express Lhx2, Isl1/2, GnRH-1 (Palaniappan et al., 2019). In birds, cells from the TN are also positive for Isl1 and Lhx2 that differ from the GnRH-1ns. A third study in mouse (Shan et al., 2020) also confirmed Isl1/2 immuno-reactivity on GnRH-1ns at early stages of GnRH neuronal development (E11.5). A subset of GnRH-1ns, positive for Wnt1Cre genetic lineage (Forni et al., 2011b), were negative for Isl1 immunoreactivity.

One prediction is that Wnt1Cre tracing, a controversial neural crest marker, and Isl1 immunoreactivity define two distinct embryonic lineages for GnRH-1ns. The rival hypothesis is that the Wnt1Cre positive subpopulation of GnRH-1ns differ in its timing and/or expression levels of Isl1 from the majority of GnRH-1ns (Forni et al., 2011b; Shan et al., 2020). Understanding the molecular cascade that establishes the genetic lineage of different cell types is a fundamental step to identify potential cellular differences between cell types and to unravel the molecular mechanisms underlying neurodevelopmental pathologies. Here, we examined which regions in the OP express Isl1/2 and analyzed Isl1 genetic lineage in different neuronal types in the nasal area of mice. We further



generated *Isl1* conditional KO mice to study the role of *Isl1* in GnRH development.

MATERIALS AND METHODS

Animals

Isl1^{fllox} (*Isl1tm2Sev/J*) (Sun et al., 2008), *Isl1^{CreERT}* (*Isl1tm1(cre/Esr1*)Krc/Sev*) (Laugwitz et al., 2005), *Isl1Cre* (*Isl1tm1(cre)Sev/J*) (Yang et al., 2006), *Rosa26tdTomato* (*B6.Cg-Gt(ROSA)26Sortm14(CAG-tdTomato)Hze/J*) (Madisen et al., 2010), and *GnRH-Cre* (*Gnrh1-cre 1Dlc/J*) (Yoon et al., 2005) mouse lines were all purchased from JAX. Genotyping was conducted following the suggested primers and protocols from JAX. Mice of either sex were used for ISH and IHC

experiments. All experiments involving mice were approved by the University at Albany Institutional Animal Care and Use Committee (IACUC).

Tamoxifen Treatment

Tamoxifen (Sigma-Aldrich), CAS # 10540–29–1, was dissolved in Corn Oil. Tamoxifen was administered once via intraperitoneal injection at indicated developmental stages. Tamoxifen was administered at 180 mg/kg based on the weight of the pregnant dam on the day of injection.

Tissue Preparation

Embryos were collected from time-mated dams where the emergence of the copulation plug was taken as E0.5. Collected

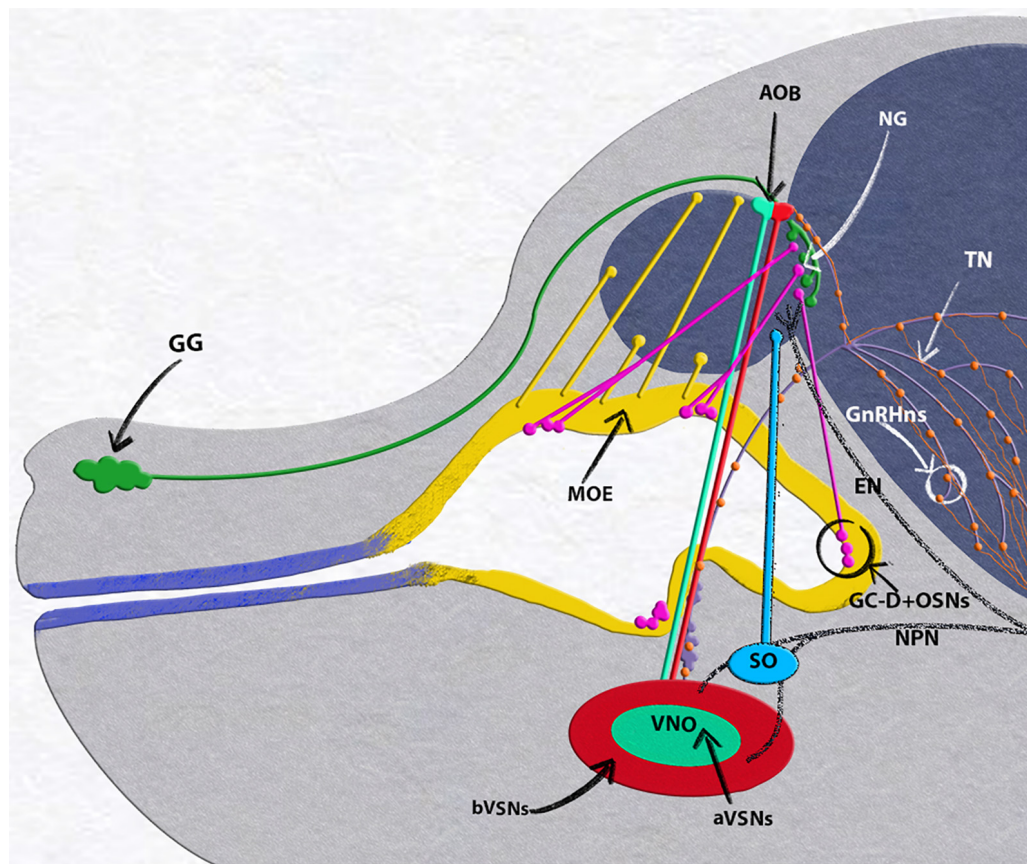


FIGURE 2 | E15.5 mouse embryo, neuronal populations in the nasal area. Gruneberg ganglion (GG, green) and GC-D+/necklace (OSNs, magenta) project to the necklace glomeruli (NG). Olfactory neurons of the main olfactory epithelium (MOE, yellow) projecting to the main olfactory bulb (MOB). Vomeronasal organ (VNO), composed of basal (bVSNs, green) and apical (aVSNs, red), projecting to anterior and posterior portions of the accessory olfactory bulb (AOB). Septal organ (SO, light blue) projecting to the ventral OB. Terminal nerve (TN, purple) projecting to the basal forebrain, GnRH-1s, orange, scattered along the terminal nerve fibers from the vomeronasal area to the basal forebrain. Trigeminal nasopalatine (NPN) and ethmoidal nerve projections (EN) drawn in dark gray.

embryos were immersion-fixed in 3.7% formaldehyde/PBS at 4°C for 3–5 h. Postnatal animals were perfused with 3.7% formaldehyde/PBS. All samples were then cryoprotected in 30% sucrose overnight, then frozen in O.C.T (Tissue-Tek), and stored at –80°C. Samples were cryosectioned using CM3050S Leica cryostat and collected on Superfrost plus slides (VWR) at 14 μm thickness for embryo's and 16 μm for post-natal tissue.

Immunohistochemistry

Primary antibodies and dilutions used in this study were: rabbit- α -Isl1 (1:1000, Abcam), mouse- α -Isl1/2 (1:100, DSHB), SW rabbit- α -GnRH-1 (1:6000, Susan Wray, NIH), goat- α olfactory marker protein (OMP; 1:4000, WAKO), rabbit- α -phospho-Histone-H3 (1:400, Cell Signaling), goat- α -Sox2 (1:400, R & D systems), rat- α -phospho-Histone-H3 (1:500, Abcam), mouse- α -Ki67 (1:500, Cell Signaling), rabbit- α -DsRed (1:1000, Clontech), goat-DsRed (1:1000, Rockland), HuC/D 8 μg/ml (Molecular Probes). Antigen retrieval was performed in a citrate buffer prior to incubation with rabbit- α -Isl1,

mouse- α -Isl1/2, rabbit- α -phospho-Histone-H3, rat- α -phospho-Histone-H3, mouse- α -Ki67. For immunoperoxidase staining procedures, slides were processed using standard protocols (Forni et al., 2013) and staining was visualized (Vectastain ABC Kit, Vector) using diaminobenzidine (DAB) in a glucose solution containing glucose oxidase to generate hydrogen peroxide; sections were counterstained with methyl green. For immunofluorescence, species-appropriate secondary antibodies were conjugated with Alexa-488, Alexa-594, or Alexa-568 (Molecular Probes and Jackson Laboratories) as specified in the legends. Sections were counterstained with 4',6'-diamidino-2-phenylindole (1:3000; Sigma-Aldrich) and coverslips were mounted with Fluoro Gel (Electron Microscopy Services). Confocal microscopy pictures were taken on a Zeiss LSM 710 microscope. Epifluorescence pictures were taken on a Leica DM4000 B LED fluorescence microscope equipped with a Leica DFC310 FX camera. Images were further analyzed using FIJ/ImageJ software. To remove auto-fluorescent blood cells in **Figure 9**, FIJ/ImageJ function image calculator was used. Each staining was replicated on at least three different animals for each genotype.

In situ Hybridization

Digoxigenin-labeled cRNA probes were prepared by *in vitro* transcription (DIG RNA labeling kit; Roche Diagnostics) from the following templates: *Isl1* from Allen Brain Atlas (Probe RP_080807_04_G12). *In situ* hybridization was performed as described (Lin et al., 2018) and visualized by immunostaining with an alkaline phosphatase conjugated anti-DIG (1:500), and NBT/BCIP developer solution (Roche Diagnostics).

Cell Quantifications

GnRH-1/*Isl1* double IHC quantifications were performed at E11.5 and E15.5 parasagittal non-serial sections on a single slide using the Rabbit- α -GnRH-1 primary and Mouse- α -*Isl1/2* primary antibodies. Embryonic co-localized cell counts on *Isl1Cre* or *Isl1Cre^{ERT}* lineage traced animals were done on E14.5 and E15.5, respectively, parasagittal non-serial whole head sections within the nasal region on a single slide where we see co-localization of both markers indicated (DsRed/*tdTomato* GnRH-1, or HuCD). Post-natal OMP cell counts were done on P8 coronal nose sections. To get the density of mature OSNs positive for constitutive *Isl1* lineage tracing at P8, number of OMP positive neurons colocalized for *tdTom* were counted in the caudal olfactory epithelium and calculated the area of the OMP positive cells within the traced epithelium. In VNO, to get the percentage of mature VSNs positive for constitutive *Isl1* lineage tracing, first OMP positive cells colocalized for *tdTom* were counted. To get the total OMP positive cells in VNO section, density of OMP cells in smaller areas of VNO was determined and extended to the total area of OMP positive cells in the VNO.

GnRH-1 cell counts were performed on *GnRH-1Cre/Islet1^{flox/flox}*, *Isl1^{CreERT/flox}*, and control at E15.5 on two immunostained non-serial slides.

Validation of Conditional *Isl1* Knockout

The *Isl1^{flox}* animals have the lox-p sites flanking exon 4 of the *Isl1* gene which codes for the homeodomain and consists of the amino acids in positions 181–240. To detect conditional loss of *Isl1^{flox}* in *GnRHCre/Is1^{flox/flox}* mutants, we performed immunolabeling using the mouse anti-*Isl1/2* (DSHB) primary antibody. This antibody recognizes the amino acids 178–349 of the *Isl1* protein and was previously shown to be unable to detect *Isl1^{flox}* (*Isl1tm2Sev/J*) mice, after Cre mediated recombination (Sun et al., 2008). However, in *Isl1^{CreERT} [Isl1tm1(cre/Esr1*)Krc/Sev]* which is null mouse model, the amino acids in positions 181–240 are maintained, therefore this null protein is still detectable in *Isl1* null cells. Since *Isl1^{CreERT}* (Laugwitz et al., 2005) and *Isl1^{flox}* alleles (Sun et al., 2008) have been targeted in different gene regions, we could not validate recombination efficiency of *Isl1^{CreERT/flox}* cKOs.

Statistical Analyses

All statistical analyses were carried out using GraphPad Prism7 software. All cell counts were averaged \pm standard error (SE) among animals of the same age and genotype. Means \pm SEs were

calculated on at least three animals per genotype. The statistical difference between genotypes and groups was determined using an unpaired student's *t*-test.

RESULTS

Isl1 Expression in Proliferative Progenitors and Neurons During Early Development of the Olfactory Pit

Using *in situ* hybridization at E11.5, we found *Isl1* mRNA expression in the more caudal region of the putative developing olfactory epithelium and proximal to the developing VNO (Figure 3A). We previously described the latter as the region where GnRH-1ns likely form and become immunoreactive (Figure 3B) (Forni et al., 2013). By pairing immunohistochemistry against *Isl1/2* and the mitotic marker phospho-histone-3 (PHH3) at E11.5, we found (Figures 3C,C') some proliferative progenitors in the apical regions of the developing pit that were also positive for *Isl1*. *Isl1/2* protein expression was consistent with the mRNA expression pattern (Figures 3A,C). However, strong *Isl1/2* immunoreactivity appeared localized in sparse nuclei ventral to the developing VNO and the putative respiratory epithelium (Figures 3C,D). Immunolabeling with anti *Isl1/2* and GnRH-1 at E11.5, E13.5, and E15.5 (Figures 3D–F'') indicated a dynamic *Isl1/2* expression across GnRH-1ns (Shan et al., 2020). In fact, we could identify at E11.5 approximately 89% (SE \pm 3.33%) of GnRH-1 + cells positive for *Isl1/2* immunoreactivity (Figures 3D–D'').

Differential Lineage Among Olfactory, Vomeronasal, and GnRH-1 Neurons

As we observed sparse and a heterogeneous distribution of *Isl1* mRNA and protein expression in the developing olfactory pit at E11.5 (Figure 3) and found *Isl1/2* protein expression with the proliferative cell marker PHH3, we decided to investigate which cells formed from the *Isl1/2* + proliferative cells. We utilized a tamoxifen inducible *Isl1Cre^{ERT}* knock-in mouse line (Laugwitz et al., 2005) mated with a sensitive Rosa-reporter (Madisen et al., 2010). *Isl1Cre^{ERT}* allows temporal control and restricts Cre mediated recombination to the time of Tamoxifen injection. Pregnant dams were treated with a single injection of Tamoxifen (180 mg/kg) at E11.5 and embryos were analyzed 4 days later (Figure 4A). At E15.5, we observed *Isl1* recombination in trigeminal nerve, inner ear, Rathke's pouch, and oral mucosa (Figures 4B,C) (Hutchinson and Eisen, 2006; Sjodal and Gunhaga, 2008; Tanaka et al., 2011; Huang et al., 2013). We also found *Isl1* tracing in the developing nasal area (Figures 4D–E'') in sparse OMP + sensory neurons of both the main olfactory and vomeronasal epithelium. Notably, *Isl1Cre* + neurons positive for the pan neuronal marker HuC/D were found at the border between the respiratory epithelium and sensory epithelium (Figures 4E,E'). We found extensive

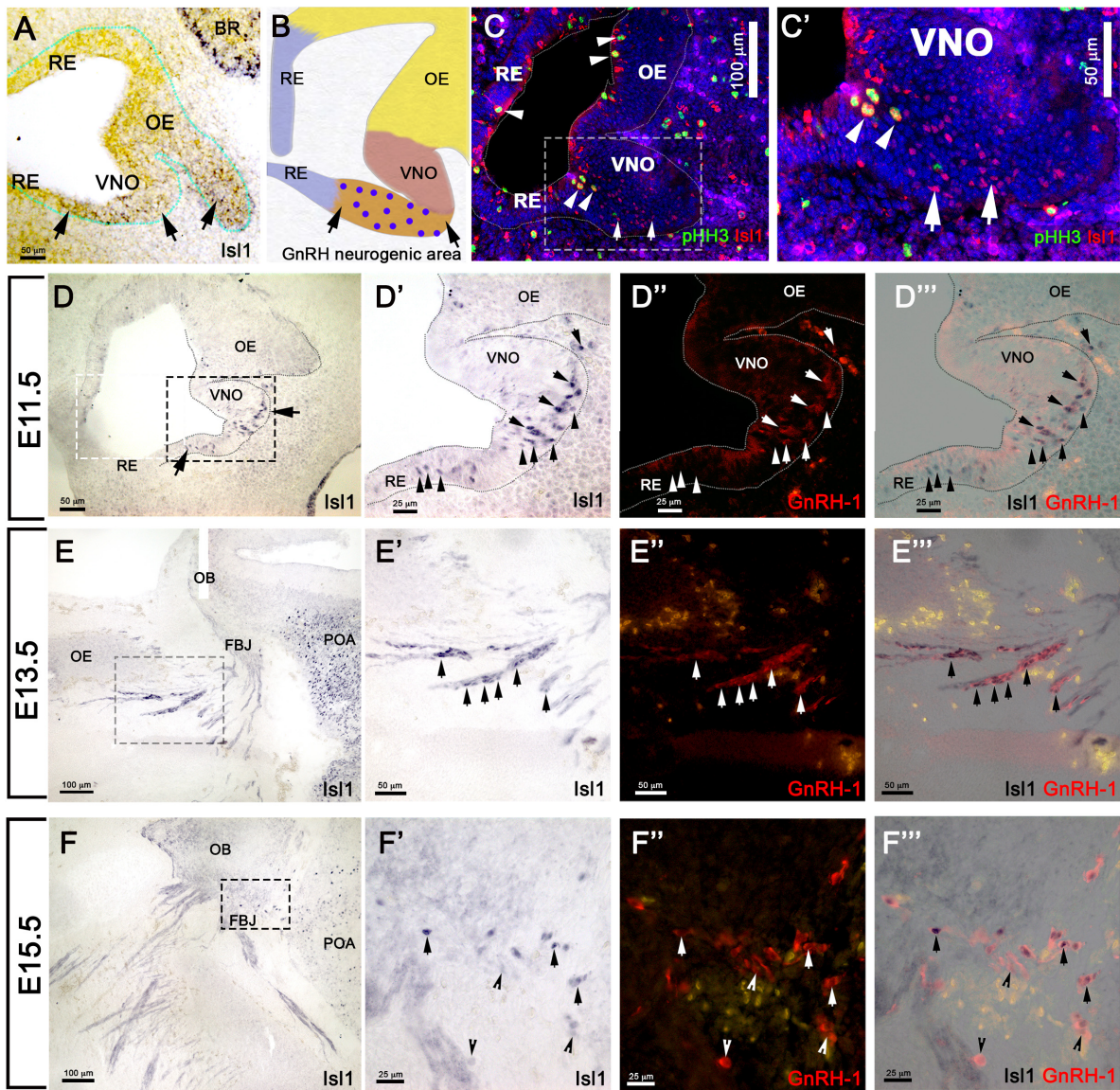


FIGURE 3 | Isl1 expression in the OP is restricted to GnRH neurons and a few other cells types. **(A)** E11.5 *in situ* hybridization anti-Isl1 mRNA shows Isl1 expression in the ventral portion of the developing olfactory pit proximal to the VNO. Arrows indicate putative GnRH neurogenic area. Only sparse cells positive for Isl1 could be detected in the OE (arrowhead). **(B)** Cartoon illustrating the putative areas giving rise to RE, OE, VNO, and the putative GnRH neurogenic area. Blue dots indicate GnRH-1ns. **(C,C')** Immunostaining anti-Isl1 (red) and the mitotic marker pHH3 (green) shows Isl1 expression in sparse proliferative cells in the apical portion of the OP (arrowheads) and in cells in the putative GnRH neurogenic area ventral to the VNO (boxed) compared to **(A,B)**. **(D)** Isl1 immunoreactivity in the putative GnRH neurogenic area (arrows, compared to **(A,B,C)**. **(D'-D''')** Isl1 expression (black) in newly formed GnRH neurons (arrows) and in GnRH-1 negative cells (arrowheads). Isl1 expression (black) in migrating GnRH-1ns in the (arrows) in the nasal area at E13.5 **(E-E''')** and in the brain at E15.5 **(F-F''')**. OE, olfactory epithelium; OB, olfactory bulb; FBJ, forebrain junction; POA, preoptic area; RE, respiratory epithelium; VNO, vomeronasal organ; BR, brain.

Cre recombination penetrance throughout the nasal respiratory epithelium (**Figures 4D,D'**).

We detected putative nasopalatine and ethmoidal trigeminal axons positive for Isl1 throughout the nasal area and tangential to the olfactory bulb (**Figures 4B-D'**). By analyzing the olfactory projections via OMP and Peripherin immunostaining in combination with anti tdTomato staining, we confirmed that Isl1Cre recombination occurred in neurons that appeared to bundle with the olfactory neurons. Notably, most Isl1Cre^{ERT}

traced axons did not appear to project to the main or accessory olfactory bulb (**Figures 4D,D'**). Analysis of the olfactory epithelium showed a very sparse colocalization between OMP and Isl1Cre mediated recombination. However, immunostaining against the pan neuronal marker HuC/D showed the presence of Isl1 + neurons within the developing olfactory epithelia (**Figures 4E,E'**). Triple immunostaining against GnRH-1, tdTomato, and the pan neuronal protein HuC/D showed that temporally controlled Isl1Cre^{ERT} recombination at

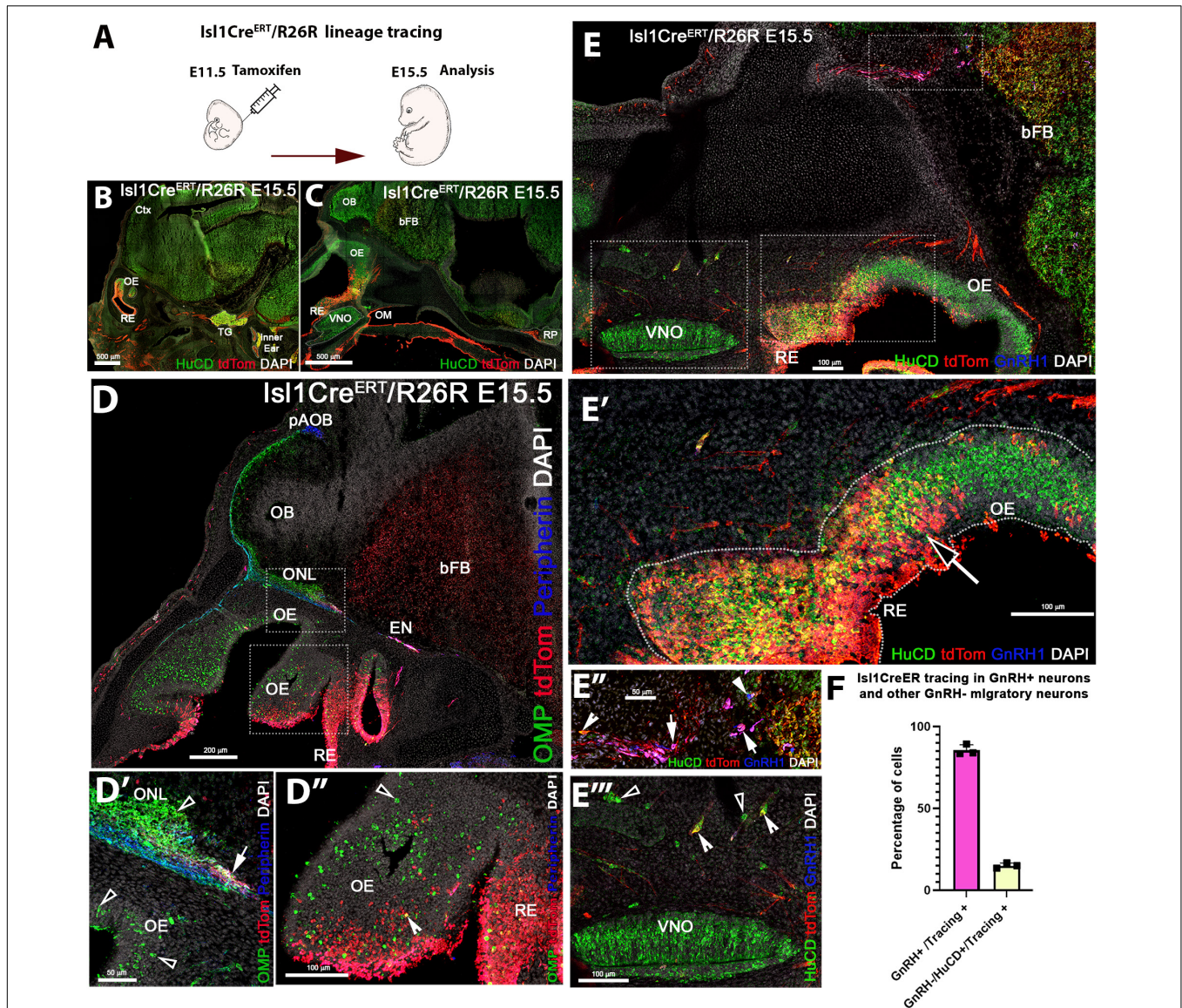
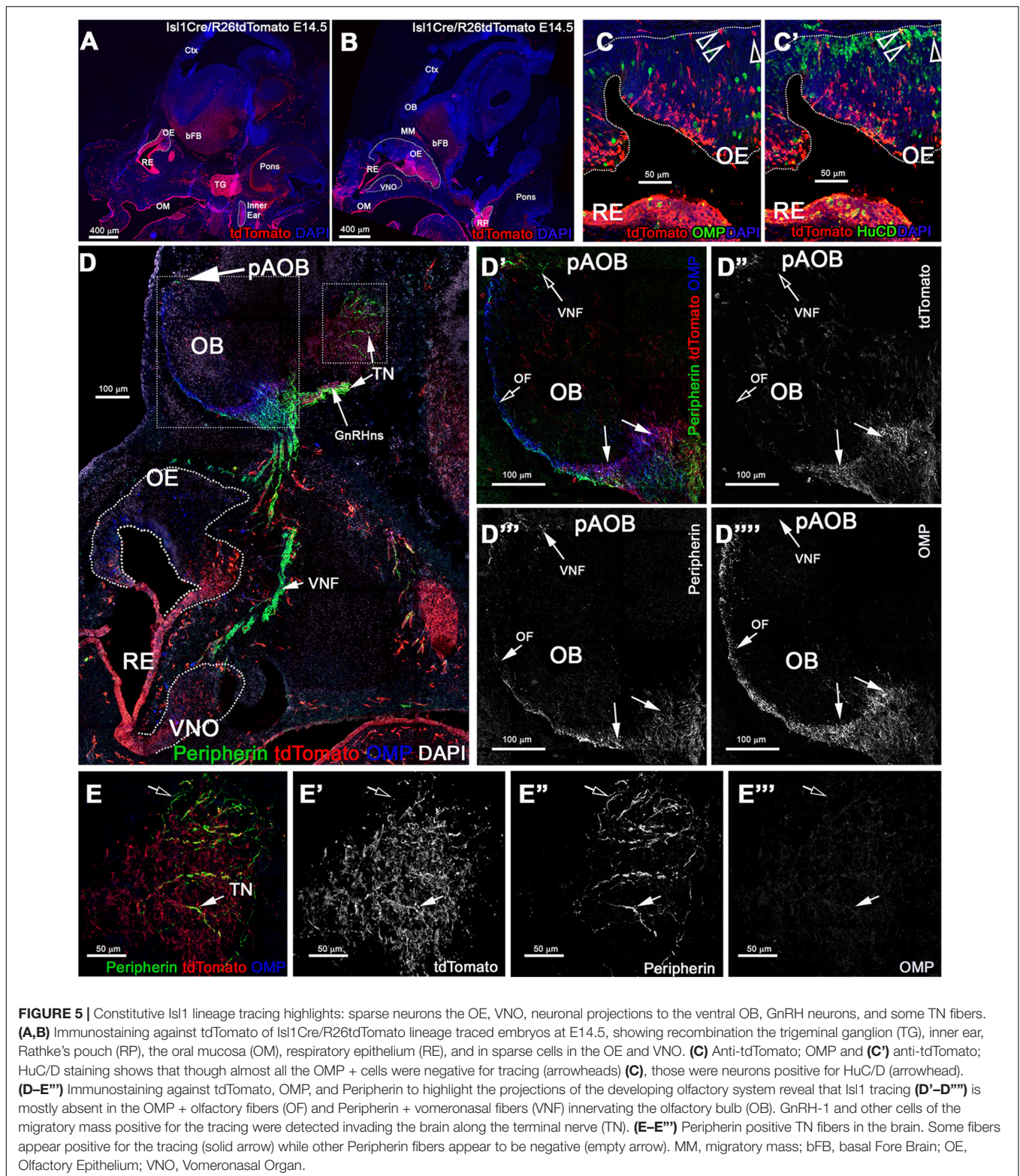


FIGURE 4 | Temporally controlled *Isl1* lineage tracing at E11.5 primarily highlights cells of the respiratory epithelium and GnRH-1ns. **(A)** Cartoon illustrating experiential strategy for *Isl1*-*CreERT*/*R26R**tdTomato* lineage tracing. Tamoxifen induction of *Cre* recombination at E11.5, analysis at E15.5. **(B,C)** HuC/D/DsRed double immunostaining shows recombination (*tdTomato*) in the trigeminal ganglion (TG), the inner ear as well as in cells of the Rathke's pouch (RP). **(D–D'')** In the developing nose recombination appears to be mostly restricted to the respiratory epithelium (RE) and ethmoidal (EN) trigeminal projections. **(D–D'')** Anti *tdTomato*; OMP; Peripherin immunostaining showed that OMP positive olfactory projections of the main olfactory bulb. Peripherin positive projections to the accessory olfactory bulb appear negative for *tdTomato* expression. However, *tdTomato* positive fibers (**D'** white arrow), likely belonging to the trigeminal/ethmoid nerve (see EN in **D**), appeared to project to the ventral OB. **(D''')** OMP and *tdTomato* immunoreactivity showed nearly complete absence of OSNs positive for *Isl1* tracing. Neurons in the olfactory area appeared mostly negative for *Isl1* lineage **D''**, sparse OMP + *tdTomato* + cells (Notched arrowhead) could be detected at the border between olfactory and respiratory epithelium, boxed area see **D'**. Pan neuronal marker HuC/D shows neurons of the developing vomeronasal organ (VNO), mostly negative for *Isl1* lineage **(E')**. HuC/D + neurons at the border between OE and RE **(E')** migratory neurons, GnRH-1ns **(E''')** and HuC/D + only **(E''')** were positive for *Isl1* tracing. **(F)** Quantification of recombination in migratory GnRH-1 + and HuC/D GnRH-1 negative neurons. OM, oral mucosa; RP, Rathke's Pouch; Ctx, cortex; OB, olfactory bulb; bFB, basal Fore Brain; pAOB, putative Accessory Olfactory Bulb.

E11.5 yielded 85% (SE \pm 1.88%) of GnRH-1ns, while only 15% (SE \pm 0.91) of the migratory (HuC/D + /GnRH-) cells were *Isl1* positive. These data suggest that *Isl1* expression at E11.5 (**Figures 3A–C**) is mostly limited to progenitors or precursors of GnRH-1ns and the subsets of other neurons of the MM.

Analysis of Constitutive *Isl1* Cre Genetic Lineage Tracing at E14.5

Tamoxifen controlled *Cre* recombination at E11.5 indicated that few neuronal progenitors and sparse neurons in the OE and VNO were positive for *Isl1* as the olfactory pit forms, while the respiratory epithelium, oral mucosa, and the



majority of the GnRH-1ns resulted expressing *Isl1*. To further perform a temporally unbiased lineage tracing for *Isl1*, we exploited a traditional *Isl1Cre* knock-in mouse line. In these mice recombination is expected to occur whenever *Isl1* is

expressed (Yang et al., 2006). We performed a *Cre/Rosa* reporter lineage analysis *Isl1^{Cre±}/R26^{tdTomato±}* at E14.5 and P8. After temporally controlled recombination (**Figure 4**), constitutively active *Isl1 Cre* at E14.5 (**Figure 5**) showed recombination in

the trigeminal nerve, cells of the inner ear (Radde-Gallwitz et al., 2004), the Rathke's pouch forming the anterior pituitary gland (Castinetti et al., 2015), the oral mucosa, and the nasal respiratory epithelium.

During gross visual observation, we noticed that more cells positive for Isl1 lineage occurred in both olfactory and vomeronasal epithelia compared to that after temporally controlled Cre activation (compared **Figures 4, 5**).

Isl1 Cre Recombination in GnRH and Terminal Nerve Neurons

At E14.5 we performed OMP, Peripherin, and tdTomato immunostaining. We observed labeled olfactory and terminal axonal projections (**Figures 5D–E**). In the olfactory system, we noticed that Isl1 Cre tracing could be seen in fibers forming bundles with the olfactory neurons after temporally controlled Isl1 Cre recombination (**Figures 5D'–D**). However, most axons positive for recombination at this stage appeared to project only to the ventral portions of the olfactory bulb with some verging on invading the basal forebrain (**Figures 5E–E**). The terminal nerve enters the brain ventral to the olfactory bulb (Taroc et al., 2017). Fibers of the putative terminal nerve associated with Isl1 + migratory GnRH-1ns. Using immunostaining against peripherin and tdTomato, we visualized Isl1 + positive cell somas and fibers of GnRH-1ns migrating on peripherin positive axons of the TN. Some putative TN's axons showed sparse positivity for tracing (**Figures 5E–E**). To confirm Isl1 Cre tracing in cells of the terminal nerve, we immunostained against the antigen Robo3, which is selectively expressed by these cells (Taroc et al., 2017). Robo3/tdTomato staining confirmed the presence of cell bodies from putative TN cells, proximal and within the developing vomeronasal organ, some of these appeared to be positive for Isl1 lineage. We also observed TN fibers, positive for Robo3, in the brain (data not shown). GnRH-1, tdTomato, and HuC/D (**Figures 6D–D**) immunostaining confirmed Isl1 lineage in virtually all GnRH-1ns (95%) ($SE \pm 0.68$), while 55% ($SE \pm 4.63$) of the HuC/D migratory neurons that were negative for GnRH-1, were actually positive for Islet1 tracing (**Figure 6E**).

Postnatal Analyses of Isl1Cre Lineage in the Nasal Cavity

During embryonic development, we observed Isl1 recombination in neurons in both olfactory and vomeronasal epithelia. So, we analyzed the pattern of constitutive Isl1 Cre recombination in postnatal animals. We performed double immunostaining against tdTomato and OMP at postnatal day 8 and noticed that most olfactory epithelium neurons did not express OMP and Isl1. However, we did find sparse neurons positive for Isl1 tracing in the most caudal ethmoid turbinates [$0.12 (\pm 0.03 \text{ SEM}) \text{ cells}/1000 \mu\text{m}^2$] (**Figures 7D–D**). Isl1Cre positive sustentacular cells were found close to the border between the respiratory epithelium and sensory olfactory epithelium in the ventral–lateral zones of the OE and along the nasal septum (S) in all the sections from rostral to caudal. At visual gross observation, we noticed more pronounced Isl1 + lineage in sustentacular cells in the caudal OE along the lateral ethmoid turbinates

(**Figures 7A–C**). These data imply spatial/regional heterogeneity in gene expression among sustentacular cells (Brann et al., 2020).

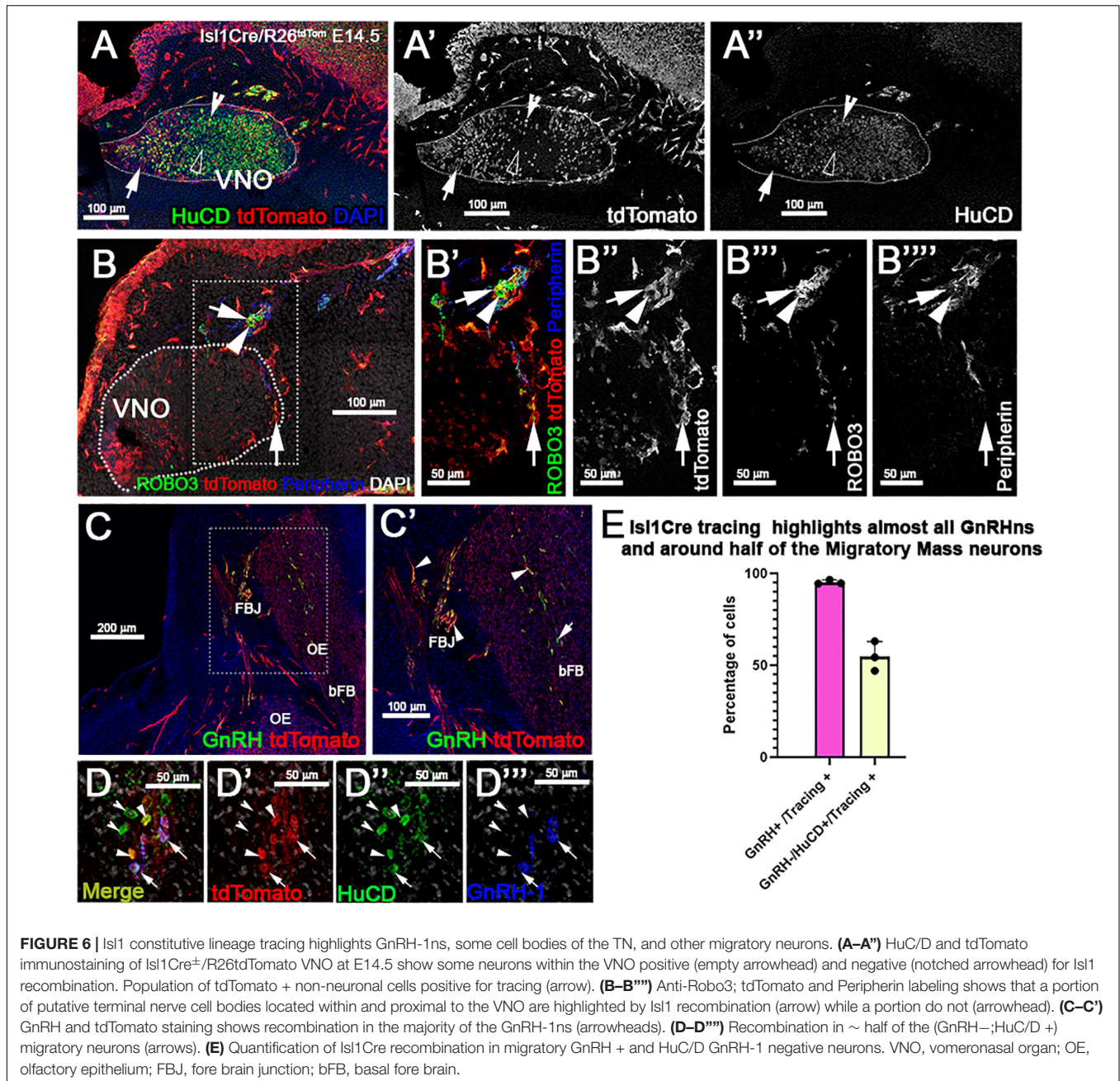
Analysis of postnatal vomeronasal epithelia showed a different scenario from that in the OE. Immunostaining against TdTom indicated Isl1 tracing in both non-sensory epithelium (NSE) and sensory epithelium of the VNO. In the sensory epithelium, staining against OMP and tdTom showed that sparse recombination in 3.74% ($\pm 1.06 \text{ SEM}$) of the neurons (**Figures 7F–F**). The vomeronasal neurons positive for tracing were variously distributed in apical and basal regions. Sox2 and tdTomato immunostaining revealed, as observed in the OE (**Figures 7E–E**), that Islet1 tracing was detectable in sustentacular cells (**Figures 7G–G**). Since constitutive Isl1 lineage showed cells positive in olfactory and vomeronasal epithelia, we further investigated if Isl1 recombination also occurred in neurons of the SO and Gruenberg ganglion (GG). By performing immunostaining anti-OMP in postnatal animals, we found that both neuronal populations were negative for lineage tracing (**Figure 8**). Immunostaining with anti-CART and -PDE2A antibodies also revealed an absence of Isl1 expression in Necklace glomeruli cells (NGCs) (data not shown).

Conditional Isl1 Loss of Function in GnRH-1ns

Isl1 is important for differentiation, cell migration, survival, and axonal targeting of neurons of the peripheral nervous system (Thor et al., 1991; Thaler et al., 2004; Sun et al., 2008). Our data revealed strong Isl1/2 expression in developing migrating GnRH-1ns (**Figures 3, 4, 6**). To test if Isl1 plays a role in GnRH-1ns migration or controls GnRH expression, we generated GnRH-1Cre/Isl1^{flox/flox} conditional mutants. Embryos were analyzed at E15.5, which is the stage at which the majority of the GnRH-1ns have already migrated in the brain (Forni et al., 2011a). Double immunostaining against Isl1/2 and GnRH confirmed detectable Isl1 ablation in 38% ($SE \pm 5.28\%$) of GnRH-1ns (**Figures 9A–B**), while Isl1 in controls was detectable in virtually all migratory GnRH-1ns. In GnRH-1Cre/Isl1^{flox/flox} conditional mutants, GnRH-1ns negative for Isl1 immunoreactivity were found in the nasal area, forebrain junction, and the brain. These data suggest that Isl1 expression is not required for GnRH-1 peptide expression nor GnRH-1 neuronal migration. Quantification of GnRH-1ns distribution in nasal area, forebrain junction, and brain indicated an overall distribution of GnRH-1ns comparable with the one of controls (**Figure 9E**).

DISCUSSION

Cellular derivatives of the OPs play central roles in respiration, chemosensory detection, sexual development, fertility, and inter- and intra-species social behaviors. Understanding the basic mechanisms that define cellular diversity and underlying normal and pathological development of the OP derivatives is of high clinical importance. Isl1 expression can occur in various neurogenic placodes (Begbie et al., 2002; Zhuang et al., 2013); however, a comprehensive analysis of Isl1 expression



remains unknown. Isl1, which is important for differentiation, cell migration, survival, and axonal targeting of neurons in the peripheral nervous system (Thor et al., 1991; Thaler et al., 2004; Sun et al., 2008), has a very high upregulation during GnRH-1 neuronal differentiation (Lund et al., 2020). So, Isl1 remained a potential suitable genetic marker to label derivatives of the OP (Shan et al., 2020). Here, we sought to trace Isl1 expression and lineage in the developing nasal area using *in situ* hybridization, immunohistochemistry (Figure 3), temporally controlled Isl1CreRT recombination (Figure 4), and constitutive Isl1Cre^{ERT} genetic lineage tracing (Figures 5–8).

GnRH-1 Lineage Tracing in the Developing Nasal Area

Using *in situ* hybridization and immunohistochemistry, we detected Isl1 expression at E11.5 in the putative GnRH neurogenic area, ventral to the developing VNO (Figures 3A–D), in newly formed GnRH-1ns and the developing olfactory epithelium (Figures 3D–F'''). At E11.5, Isl1 immunoreactivity occurred in 89% (±3.33%) of GnRH cells, in line with published reports (Shan et al., 2020). However, histochemistry at E13.5 and E15.5 showed strong Isl1/2 immunoreactivity in virtually all GnRH-1ns, suggesting that Isl1 expression is not limited to specific subpopulations of GnRH cells (Shan et al., 2020). These

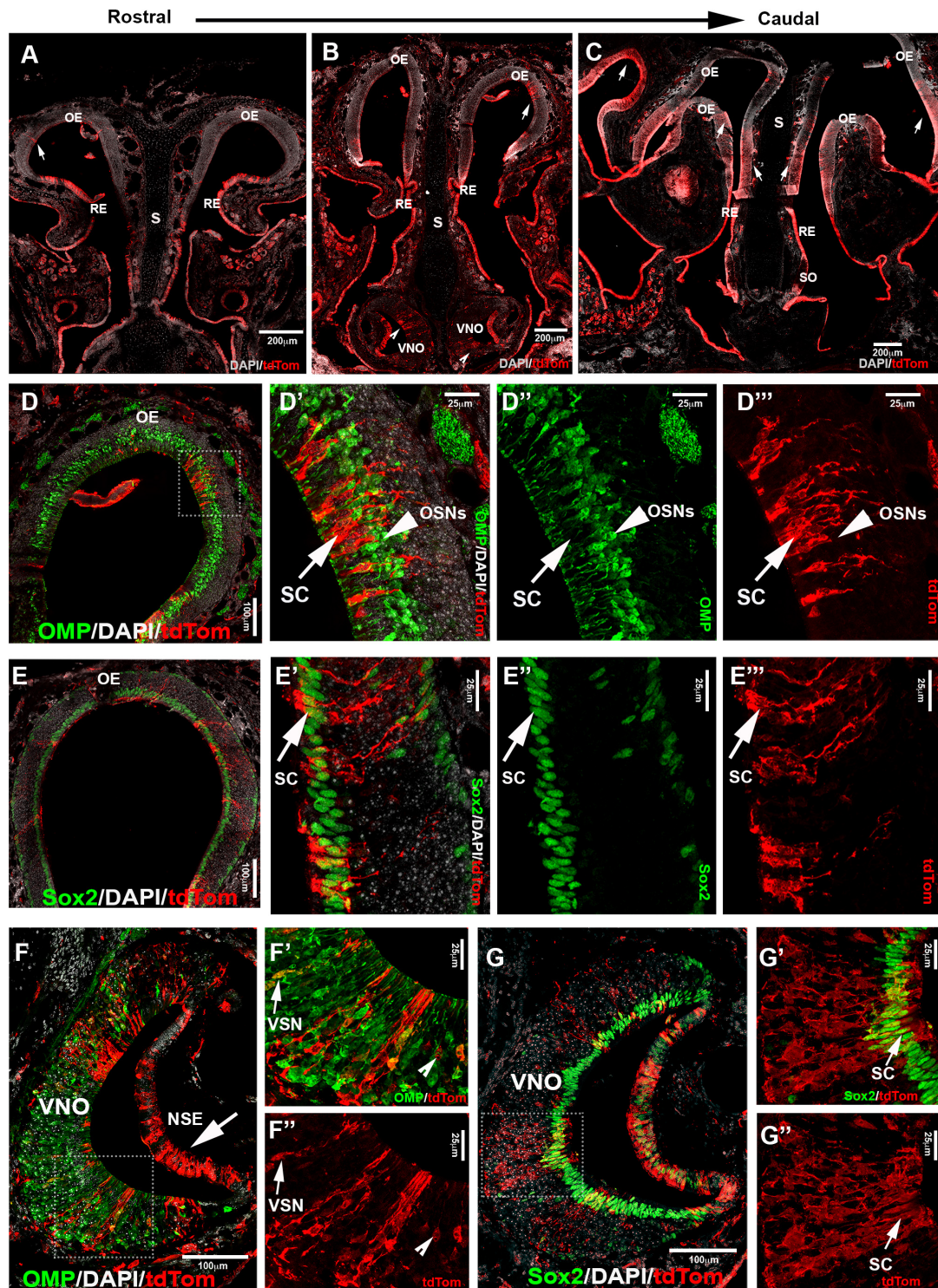


FIGURE 7 | Lineage tracing of Isl1 positive cells postnatally highlights neuronal and non-neuronal cells in OE and VNE. **(A–C)** Immunofluorescence against tdTom showing Isl1 tracing in olfactory epithelium (OE) from rostral toward the caudal ethmoid turbinates. Arrows **(A,B,C)** show tracing in OE. **(B)** Notched arrowheads show tracing in VNO. **(D–D''')** Double immunofluorescence against OMP (green) and tdTom (red) shows no colocalization in neurons of the OE. **(E–E''')** Double immunofluorescence against Sox2 (green) and tdTom (red) shows Isl1Cre tracing (arrow marks) in the sustentacular cells of the OE. Sox2 is present in both globose basal cells that are present in the base of the OE and sustentacular cells in the upper layers of the OE. **(F)** Double immunofluorescence against OMP (green) and tdTom (red) shows Isl1 tracing in both non-sensory epithelium (NSE—arrow mark) and sensory epithelium of the VNO. **(F',F'')** Arrow marks show colocalized mature vomeronasal neurons (VSNs) and notched arrow heads show traced neurons that are not labeled with OMP. **(G–G''')** Double immunofluorescence against Sox2 (green) and tdTom (red) shows Isl1 tracing in sustentacular cells in the VNO. S, septum; SO, septal organ; SC, sustentacular cells; OSNs, olfactory sensory neurons.

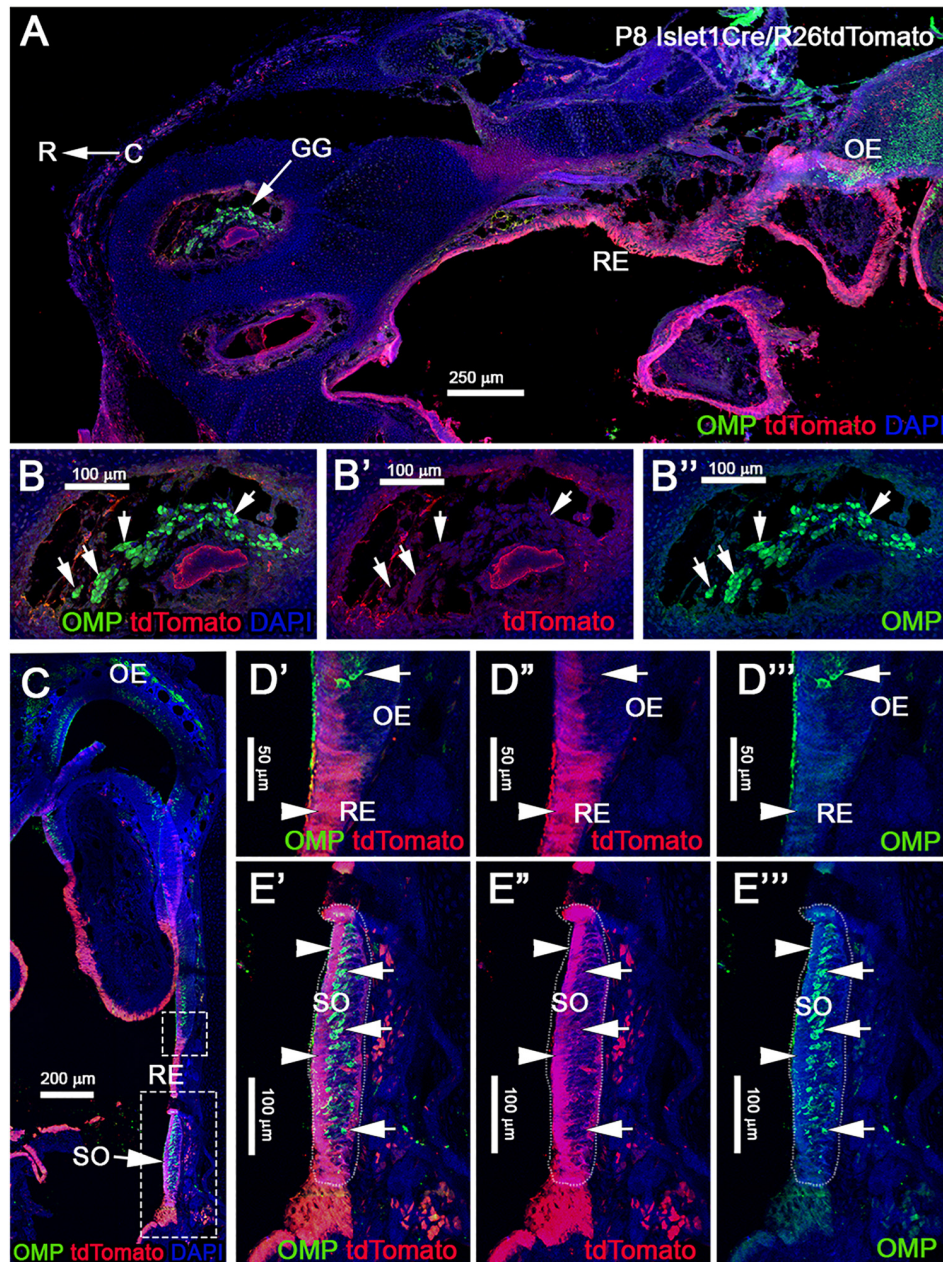
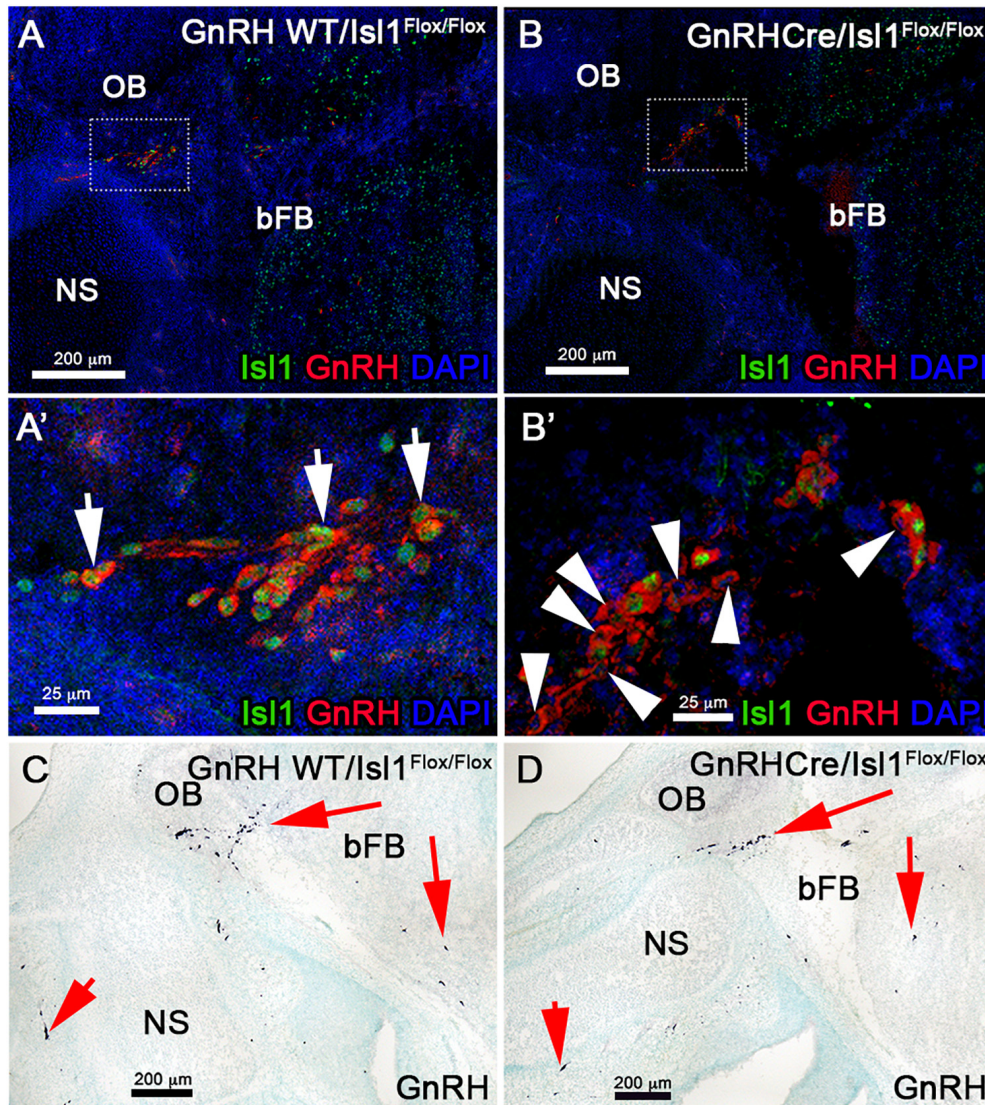


FIGURE 8 | Post-natal *Isl1* constitutive lineage tracing is not expressed in other nasal sensory neurons. **(A)** *Isl1*Cre/*R26tdTomato* P8 parasagittal section of the nose immunostained against OMP and tdTomato shows that *Isl1* recombination is limited to the respiratory epithelium even in post-natal stages. Neuronal sensory populations, such as the Gruenberg Ganglion (GG) **(B–B’)**, is negative for recombination. **(C)** Coronal view of *Isl1*Cre/*R26tdTomato* at P8, stained against OMP and tdTomato shows *Isl1* tracing restricted to the non-sensory cells and cells of the respiratory epithelium. **(D–D’)** Magnification from **C** of the border between olfactory and respiratory epithelium shows *Isl1*Cre tracing restricted to the respiratory epithelium (arrowhead), while OMP + neurons are negative (arrow). **(E–E’)** Septal organ (SO) from **C** indicates *Isl1* recombination is restricted to the non-sensory (arrowheads) cells, while OMP + neurons are negative (arrows). R, rostral; C, caudal; RE, respiratory epithelium; OE, olfactory epithelium.

data suggest a dynamic expression of *Isl1* with more GnRH-1 cells positive across development.

At E11.5 we also found the existence of proliferative cells positive for *Isl1* in the developing olfactory pit. Tamoxifen controlled *Isl1*Cre^{ERT} tracing at E11.5 showed *Isl1* lineage in putative GnRH progenitors/newly formed GnRH-1ns, cells

of the respiratory epithelium, few proliferative progenitors in the developing olfactory pit, neurons at the border between respiratory epithelium and developing olfactory epithelium and sparse neuronal (HuC/D+) cells in the OE and VNO. Notably in this experiment we analyzed *Isl1*Cre^{ERT}/*R26R* recombination 4 days after Tam treatment. This means that,



Isl1 conditional ablation does not affect number or distribution of GnRH1ns

E

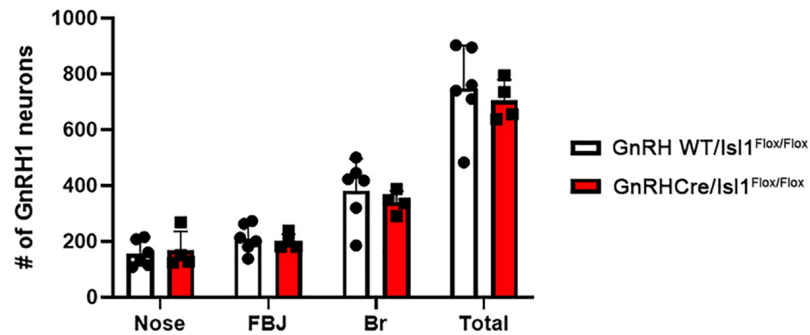


FIGURE 9 | Conditional loss of Isl1 in GnRH-1ns has no effect in their migration or development. Isl1/2 and GnRH double IF on E15.5 WT (**A–A'**), where all GnRH-1ns express Isl1/2 (arrows) and cKO (**B–B'**) sections show that some GnRH-1ns lose the expression of Isl1 (arrowheads). (**C,D**) Immunohistochemistry of GnRH-1 on WT and cKO sections shows comparable distribution of cells positive for GnRH-1ns. (**E**) Quantification of cKO shows no changes in the number or distribution of GnRH-1ns. NS, nasal septum; OB, olfactory bulb; bFB, basal forebrain.

when we observed the histological samples, we identified either cells that expressed *Isl1* at the moment of Tam injection or cells that derived from progenitors expressing *Isl1* at time of Tam injection.

In line with what observed after temporally Tam controlled recombination at E11.5, constitutively active *Isl1Cre* recombination showed that, during embryonic development (Figures 5, 6), *Isl1* tracing highlights neurons in OE proximal to the border with RE, neurons in the vomeronasal organ, cells of the RE, GnRH-1ns, migratory neurons negative for GnRH, and sustentacular cells in olfactory and vomeronasal organ.

These data indicate that *Isl1* expression/lineage is limited to specific subsets of olfactory placodal derivatives. In contrast to prior observations during embryonic development, *Isl1Cre* recombination analysis of postnatal *Isl1Cre/R26R* mice showed only sparse neurons positive for *Isl1* tracing in the most caudal regions of the olfactory sensory epithelium, while cells positive for *Isl1* tracing were still found in the VNO, respiratory epithelium, and in sustentacular cells of both OE and VNO (Figure 7). No *Isl1* expression or lineage was in GC neurons and GG (Figure 8). These data suggest that *Isl1* positive neurons in the OE at the border with the RE during embryonic development (Figures 4, 5) either migrated out of the epithelium as a part of the MM or died, even though we could still detect *Isl1* expression/lineage in some vomeronasal organ neurons (Figures 7F–F’). So, we further defined the fate of the *Isl1* neurons detectable in the OE during embryonic development. During embryonic development, we could also detect axonal projections positive for *Isl1* traversing through the nasal area (Figures 4, 5). Some axonal projections likely belonged to the nasopalatine projections of the trigeminal nerve (Figures 3–5). Although both *Isl1^{CreERT}* and *Isl1Cre* induced recombination in *Peripherin +* fibers projected to the ventral OB, the majority of *OMP +* fibers projecting to the MOB and AOB appeared negative for *Isl1* tracing (Figures 4, 5). We did not pursue a detailed analysis of olfactory projections in postnatal animals, due to technical challenges in tracing *Isl1* recombination in mitral cells of the MOB.

Isl1 in the GnRH-1 System

During embryonic development, GnRH-1ns migrate from the developing olfactory pit into the hypothalamus. Once in the preoptic area, GnRH neurons (GnRH-1ns) control the hypothalamic–pituitary–gonadal hormonal axis and reproductive development. Defective GnRH-1 release is the cause of HH, a condition that negatively impacts normal body development, social interactions, the ability to procreate, and physical performances (Burmeister et al., 2005; Yin and Gore, 2006; Maruska and Fernald, 2011; Zhang et al., 2013). HH associated with congenital anosmia (impairment of the sense of smell) is clinically defined as Kallmann syndrome (Kallmann, 1944; Legouis et al., 1991; Guioli et al., 1992; Hardelin et al., 1992; Incerti et al., 1992; Dode et al., 2003; Pitteloud et al., 2007). Though postnatal development of the olfactory system has been extensively studied, we still ignore many aspects regarding early development of the olfactory pit derivatives.

Previous studies in chick and mice indicate that soon after the OPs form they give rise to migratory olfactory pioneer neurons, and to several other neuronal populations including the terminal nerve cells and the GnRH-1ns. Placodal derived migratory neurons and the neural crest derived olfactory ensheathing cells form the MM (Barraud et al., 2013, 2010).

We previously showed that the fibers of the terminal nerve, upon which the GnRH-1ns migrate, are distinct from the OSN and VSN (Taroc et al., 2017, 2019, 2020). What progenitors give rise to the GnRH neurons, and what transcription factors control their onset are still open questions. Moreover, if what we define as GnRH neurons is one homogenous neuronal population is also a matter of debate.

Lineage tracing at different developmental stages suggests strong and consistent *Isl1* expression in GnRH-1ns and cells of the MM (Figures 3, 4, 6). While the terminal nerve that projects from the vomeronasal area to the basal forebrain appeared to have heterogeneous *Isl1* expression/genetic lineage tracing (Figure 6), *Isl1* has been reported to be important in neuronal differentiation, cell migration, survival, and axonal targeting of various neuronal types (Thor et al., 1991; Thaler et al., 2004; Sun et al., 2008). The consistent *Isl1/2* expression in developing and migratory GnRH-1ns (Figures 3, 4, 6), which is conserved from fish to humans prompted us to test its developmental role.

We first made an attempt to conditionally KO *Isl1*, which as a whole KO is embryonic lethal, by mating *Isl1^{CreERT}* mice (Figure 4), which are *Isl1^{null}* heterozygous, with *Isl1^{flox}*. After Tamoxifen injection at E11.5, we analyzed *Isl1^{CreERT/flox}* mice and controls at E15.5 (as in Figure 4). After Tamoxifen treatment, *Isl1^{CreERT}* extensively recombines in the developing GnRH-1ns (Figure 4). Surprisingly Tam + *Isl1^{CreERT/Isl1^{flox}}* embryos did not show any obvious phenotype related to GnRH-1ns (Supplementary Material). However, for this model, we could not verify the efficiency of recombination because antibodies unable to detect the floxed *Isl1* truncated protein were still recognizing the *Isl1^{CreERT}* protein product (see section “Materials and Methods”). For this reason, we report these as supplementary observations. In order to further test the role of *Isl1* in GnRH-1 neuronal development, we generated *GnRH-1Cre/Isl1^{flox/flox}* conditional mutants. Here, we could document complete loss of *Isl1* immunoreactivity in around ~40% of GnRH-1ns (Figure 9). Notably most of the anti *Isl1* Abs have some level of cross reactivity with *Isl2*, therefore we performed *in situ* hybridization against exon 4 of *Isl1* paired with anti GnRH-1 immunofluorescent staining (not shown). These experiments suggest similar penetrance of recombination as indicated by IF. Notably, also in *GnRH-1Cre/Isl1^{flox/flox}* mutants, we did not observe obvious defects in GnRH-1 neuronal migration nor in GnRH-1 expression (Figure 9). In fact, GnRH-1ns negative for *Isl1* were found in both nasal area and brain. Total number and overall distribution of GnRH-1 was comparable to controls. These data suggest that *Isl1* alone is not necessary for GnRH-1 expression or neuronal migration. We believe that our conditional *Isl1KO* might partially compensate *Isl1* loss-of-function through *Isl2* expression. Notably, *Isl1* and *Isl2* have been shown to be required for the expression of neuropilin-1

(Nrp1) (Lee et al., 2015). Moreover, it was recently demonstrated that selective loss of Nrp1 in GnRH-1ns leads to a total increase in the number of GnRH-1ns in mouse (Vanacker et al., 2020). In line with these observations in our Isl1^{CreERT/Flox} cKO embryos, we observed a trend with an increase in the total number of immunoreactive GnRH-1ns (Supplementary Figure S1). Since loss of Nrp1 expression is more dramatic in Isl1/Isl2 double knockouts (Lee et al., 2015), we predict that Isl1/Isl2 double knockouts could have increased number of GnRH-1ns as reported for Nrp1 null mice (Vanacker et al., 2020).

CONCLUSION

Our data indicate very selective expression of Isl1 in neurons forming in the OP including the GnRH-1ns, various migratory neuronal populations and some cells in the VNO, terminal nerve and sustentacular cells on the more medial and lateral portions of the OE. Isl-1 immunoreactivity and genetic tracing suggest that Isl-1 expression, though dynamic, is common feature for virtually all GnRH-1ns (Shan et al., 2020) and several other neurons of the MM. If all these early migratory neurons derive from similar pre-placodal subregions should be further investigated. Performing GnRH-1ns specific Isl1 ablation in GnRH-1ns we did not detect obvious cell specification, differentiation, survival, or migratory defects (Shan et al., 2020) at embryonic development stages suggesting a dispensable role for Isl1 in GnRH neurons.

Our results leave open the question of what is the physiological role of this transcription factor in murine GnRH-1ns development and function. Further studies focused on Isl1 role in postnatal developmental and fertility can give definitive insights.

DATA AVAILABILITY STATEMENT

All datasets presented in this study are included in the article/Supplementary Material.

REFERENCES

- Aguillon, R., Batut, J., Subramanian, A., Madelaine, R., Dufourcq, P., Schilling, T. F., et al. (2018). Cell-type heterogeneity in the early zebrafish olfactory epithelium is generated from progenitors within preplacodal ectoderm. *eLife* 7:e32041. doi: 10.7554/eLife.32041
- Bailey, A. P., and Streit, A. (2006). Sensory organs: making and breaking the pre-placodal region. *Curr. Top. Dev. Biol.* 72, 167–204. doi: 10.1016/s0070-2153(05)72003-2
- Balashubramanian, R., Dwyer, A., Seminara, S. B., Pitteloud, N., and Kaiser, U. B. (2010). Human GnRH deficiency: a unique disease model to unravel the ontogeny of GnRH neurons. *Neuroendocrinology* 92, 81–99. doi: 10.1159/000314193
- Barraud, P., Seferiadis, A. A., Tyson, L. D., Zwart, M. F., Szabo-Rogers, H. L., Ruhrberg, C., et al. (2010). Neural crest origin of olfactory ensheathing glia. *Proc. Natl. Acad. Sci. U.S.A.* 107, 21040–21045. doi: 10.1073/pnas.1012248107
- Barraud, P., St John, J. A., Stolt, C. C., Wegner, M., and Baker, C. V. (2013). Olfactory ensheathing glia are required for embryonic olfactory axon targeting

ETHICS STATEMENT

The animal study was reviewed and approved by the Institutional Animal Care and Use Committee (IACUC).

AUTHOR CONTRIBUTIONS

ET set the mouse mating, collected samples, prepared histological samples, performed immunostaining and imaging, and analyzed data at embryonic developmental stages. RK prepared histological samples and performed immunostaining and analyses of postnatal animals. ET and PF designed the experiments, wrote the article, and prepared figure panels. All authors contributed to the article and approved the submitted version.

FUNDING

Research reported in this publication was supported by the Eunice Kennedy Shriver National Institute of Child Health and Human Development of the National Institutes of Health under the Awards R15-HD096411 (PF) and R01-HD097331/HD/NICHD (PF), and by the National Institute of Deafness and Other Communication Disorders of the National Institutes of Health under the Award R01-DC017149 (PF).

SUPPLEMENTARY MATERIAL

The Supplementary Material for this article can be found online at: <https://www.frontiersin.org/articles/10.3389/fphys.2020.601923/full#supplementary-material>

Supplementary Figure 1 | Isl1^{CreERT}/Isl1^{Flox} conditional knockout at E11.5 does not affect GnRH1ns. GnRH IHC on WT (A) and cKO (B) sections show that between each genotype the distribution of GnRH-1ns looks similar. (C) Quantification of the number of GnRH-1ns in whole embryo heads shows no significant regional changes or in total cell number.

- and the migration of gonadotropin-releasing hormone neurons. *Biol. Open* 2, 750–759. doi: 10.1242/bio.20135249
- Begbie, J., Ballivet, M., and Graham, A. (2002). Early steps in the production of sensory neurons by the neurogenic placodes. *Mol. Cell. Neurosci.* 21, 502–511. doi: 10.1006/mcne.2002.1197
- Brann, D. H., Tsukahara, T., Weinreb, C., Lipovsek, M., Van den Berge, K., Gong, B., et al. (2020). Non-neuronal expression of SARS-CoV-2 entry genes in the olfactory system suggests mechanisms underlying COVID-19-associated anosmia. *Sci. Adv.* 6:eabc5801. doi: 10.1126/sciadv.abc5801
- Brown, J. W. (1987). The nervus terminalis in insectivorous bat embryos and notes on its presence during human ontogeny. *Ann. N.Y. Acad. Sci.* 519, 184–200. doi: 10.1111/j.1749-6632.1987.tb36297.x
- Brugmann, S. A., and Moody, S. A. (2005). Induction and specification of the vertebrate ectodermal placodes: precursors of the cranial sensory organs. *Biol. Cell.* 97, 303–319. doi: 10.1042/bc20040515
- Burmeister, S. S., Jarvis, E. D., and Fernald, R. D. (2005). Rapid behavioral and genomic responses to social opportunity. *PLoS Biol.* 3:e363. doi: 10.1371/journal.pbio.0030363

- Castinetti, F., Brinkmeier, M. L., Mortensen, A. H., Vella, K. R., Gergics, P., Brue, T., et al. (2015). ISL1 is necessary for maximal thyrotrope response to hypothyroidism. *Mol. Endocrinol.* 29, 1510–1521. doi: 10.1210/me.2015-1192
- Cattanach, B. M., Iddon, C. A., Charlton, H. M., Chiappa, S. A., and Fink, G. (1977). Gonadotrophin-releasing hormone deficiency in a mutant mouse with hypogonadism. *Nature* 269, 338–340. doi: 10.1038/269338a0
- Cau, E., Casarosa, S., and Guillemot, F. (2002). Mash1 and Ngn1 control distinct steps of determination and differentiation in the olfactory sensory neuron lineage. *Development* 129, 1871–1880.
- Cau, E., Gradwohl, G., Casarosa, S., Kageyama, R., and Guillemot, F. (2000). Hes genes regulate sequential stages of neurogenesis in the olfactory epithelium. *Development* 127, 2323–2332.
- Cau, E., Gradwohl, G., Fode, C., and Guillemot, F. (1997). Mash1 activates a cascade of bHLH regulators in olfactory neuron progenitors. *Development* 124, 1611–1621.
- Chen, B., Kim, E. H., and Xu, P. X. (2009). Initiation of olfactory placode development and neurogenesis is blocked in mice lacking both Six1 and Six4. *Dev. Biol.* 326, 75–85. doi: 10.1016/j.ydbio.2008.10.039
- Cuschieri, A., and Bannister, L. H. (1975a). The development of the olfactory mucosa in the mouse: electron microscopy. *J. Anat.* 119, 471–498.
- Cuschieri, A., and Bannister, L. H. (1975b). The development of the olfactory mucosa in the mouse: light microscopy. *J. Anat.* 119, 277–286.
- Dode, C., Levilliers, J., Dupont, J. M., De Paep, A., Le Du, N., Soussi-Yanicostas, N., et al. (2003). Loss-of-function mutations in FGFR1 cause autosomal dominant Kallmann syndrome. *Nat. Genet.* 33, 463–465. doi: 10.1038/ng1122
- Donner, A. L., Episkopou, V., and Maas, R. L. (2007). Sox2 and Pou2f1 interact to control lens and olfactory placode development. *Dev. Biol.* 303, 784–799. doi: 10.1016/j.ydbio.2006.10.047
- Fornaro, M., Geuna, S., Fasolo, A., and Giacobini-Robecchi, M. G. (2003). HuC/D confocal imaging points to olfactory migratory cells as the first cell population that expresses a post-mitotic neuronal phenotype in the chick embryo. *Neuroscience* 122, 123–128. doi: 10.1016/j.neuroscience.2003.07.004
- Fornaro, M., Raimondo, S., Lee, J. M., and Giacobini-Robecchi, M. G. (2007). Neuron-specific Hu proteins sub-cellular localization in primary sensory neurons. *Ann. Anat.* 189, 223–228. doi: 10.1016/j.aanat.2006.11.004
- Forni, P. E., Bharti, K., Flannery, E. M., Shimogori, T., and Wray, S. (2013). The indirect role of fibroblast growth factor-8 in defining neurogenic niches of the olfactory/GnRH systems. *J. Neurosci.* 33, 19620–19634. doi: 10.1523/jneurosci.3238-13.2013
- Forni, P. E., Fornaro, M., Guenette, S., and Wray, S. (2011a). A role for FE65 in controlling GnRH-1 neurogenesis. *J. Neurosci.* 31, 480–491. doi: 10.1523/jneurosci.4698-10.2011
- Forni, P. E., Taylor-Burds, C., Melvin, V. S., Williams, T., and Wray, S. (2011b). Neural crest and ectodermal cells intermix in the nasal placode to give rise to GnRH-1 neurons, sensory neurons, and olfactory ensheathing cells. *J. Neurosci.* 31, 6915–6927. doi: 10.1523/jneurosci.6087-10.2011
- Forni, P. E., and Wray, S. (2015). GnRH, anosmia and hypogonadotropic hypogonadism—where are we? *Front. Neuroendocrinol.* 36:165–177. doi: 10.1016/j.yfrne.2014.09.004
- Greer, P. L., Bear, D. M., Lassance, J. M., Bloom, M. L., Tsukahara, T., Pashkovski, S. L., et al. (2016). A family of non-GPCR chemosensors defines an alternative logic for mammalian olfaction. *Cell* 165, 1734–1748. doi: 10.1016/j.cell.2016.05.001
- Gruneberg, H. (1973). A ganglion probably belonging to the N. terminalis system in the nasal mucosa of the mouse. *Z. Anat. Entwicklungsgesch.* 140, 39–52. doi: 10.1007/bf00520716
- Guioli, S., Incerti, B., Zanaria, E., Bardoni, B., Franco, B., Taylor, K., et al. (1992). Kallmann syndrome due to a translocation resulting in an X/Y fusion gene. *Nat. Genet.* 1, 337–340. doi: 10.1038/ng0892-337
- Hardelin, J. P., Levilliers, J., del Castillo, I., Cohen-Salmon, M., Legouis, R., Blanchard, S., et al. (1992). X chromosome-linked Kallmann syndrome: stop mutations validate the candidate gene. *Proc. Natl. Acad. Sci. U.S.A.* 89, 8190–8194. doi: 10.1073/pnas.89.17.8190
- Hilal, E. M., Chen, J. H., and Silverman, A. J. (1996). Joint migration of gonadotropin-releasing hormone (GnRH) and neuropeptide Y (NPY) neurons from olfactory placode to central nervous system. *J. Neurobiol.* 31, 487–502. doi: 10.1002/(sici)1097-4695(199612)31:4<487::aid-neu8>3.0.co;2-5
- Huang, M., Kantardzhieva, A., Scheffer, D., Liberman, M. C., and Chen, Z. Y. (2013). Hair cell overexpression of Islet1 reduces age-related and noise-induced hearing loss. *J. Neurosci.* 33, 15086–15094. doi: 10.1523/jneurosci.1489-13.2013
- Hutchinson, S. A., and Eisen, J. S. (2006). Islet1 and Islet2 have equivalent abilities to promote motoneuron formation and to specify motoneuron subtype identity. *Development* 133, 2137–2147. doi: 10.1242/dev.02355
- Incerti, B., Guioli, S., Pragliola, A., Zanaria, E., Borsani, G., Tonlorenzi, R., et al. (1992). Kallmann syndrome gene on the X and Y chromosomes: implications for evolutionary divergence of human sex chromosomes. *Nat. Genet.* 2, 311–314. doi: 10.1038/ng1292-311
- Jennes, L. (1987). The nervus terminalis in the mouse: light and electron microscopic immunocytochemical studies. *Ann. N.Y. Acad. Sci.* 519, 165–173. doi: 10.1111/j.1749-6632.1987.tb36295.x
- Jin, Z. W., Cho, K. H., Shibata, S., Yamamoto, M., Murakami, G., and Rodriguez-Vazquez, J. F. (2019). Nervus terminalis and nerves to the vomeronasal organ: a study using human fetal specimens. *Anat. Cell. Biol.* 52, 278–285. doi: 10.5115/acb.19.020
- Kallmann, F. J. (1944). The genetic aspects of primary eunuchoidism. *J. Ment. Defic.* 48, 203–236.
- Katoh, H., Shibata, S., Fukuda, K., Sato, M., Satoh, E., Nagoshi, N., et al. (2011). The dual origin of the peripheral olfactory system: placode and neural crest. *Mol. Brain* 4:34. doi: 10.1186/1756-6606-4-34
- Larsell, O. (1950). The nervus terminalis. *Ann. Otol. Rhinol. Laryngol.* 59, 414–438.
- Laugwitz, K. L., Moretti, A., Lam, J., Gruber, P., Chen, Y., Woodard, S., et al. (2005). Postnatal Isl1+ cardioblasts enter fully differentiated cardiomyocyte lineages. *Nature* 433, 647–653. doi: 10.1038/nature03215
- Lee, H., Kim, M., Kim, N., Macfarlan, T., Pfaff, S. L., Mastick, G. S., et al. (2015). Slit and Semaphorin signaling governed by Islet transcription factors positions motor neuron somata within the neural tube. *Exp. Neurol.* 269, 17–27. doi: 10.1016/j.expneurol.2015.03.024
- Legouis, R., Hardelin, J. P., Levilliers, J., Claverie, J. M., Compain, S., Wunderle, V., et al. (1991). The candidate gene for the X-linked Kallmann syndrome encodes a protein related to adhesion molecules. *Cell* 67, 423–435. doi: 10.1016/0092-8674(91)90193-3
- Lin, J. M., Taroc, E. Z. M., Frias, J. A., Prasad, A., Catizone, A. N., Sammons, M. A., et al. (2018). The transcription factor Tfp2e/AP-2epsilon plays a pivotal role in maintaining the identity of basal vomeronasal sensory neurons. *Dev. Biol.* 441, 67–82. doi: 10.1016/j.ydbio.2018.06.007
- Lund, C., Yellapragada, V., Vuoristo, S., Balboa, D., Trova, S., Allet, C., et al. (2020). Characterization of the human GnRH neuron developmental transcriptome using a GNRH1-TdTomato reporter line in human pluripotent stem cells. *Dis. Model. Mech.* 13:dmm040105. doi: 10.1242/dmm.040105
- Luo, M. (2008). The necklace olfactory system in mammals. *J. Neurogenet.* 22, 229–238. doi: 10.1080/01677060802340228
- Ma, M., Grosmaître, X., Iwema, C. L., Baker, H., Greer, C. A., and Shepherd, G. M. (2003). Olfactory signal transduction in the mouse septal organ. *J. Neurosci.* 23, 317–324. doi: 10.1523/jneurosci.23-01-00317.2003
- Madisen, L., Zwingman, T. A., Sunkin, S. M., Oh, S. W., Zariwala, H. A., Gu, H., et al. (2010). A robust and high-throughput Cre reporting and characterization system for the whole mouse brain. *Nat. Neurosci.* 13, 133–140. doi: 10.1038/nn.2467
- Mamasuew, K., Hofmann, N., Breer, H., and Fleischer, J. (2011). Grueneberg ganglion neurons are activated by a defined set of odorants. *Chem. Senses.* 36, 271–282. doi: 10.1093/chemse/bjq124
- Maruska, K. P., and Fernald, R. D. (2011). Social regulation of gene expression in the hypothalamic-pituitary-gonadal axis. *Physiology* 26, 412–423. doi: 10.1152/physiol.00032.2011
- Matsuo, T., Rossier, D. A., Kan, C., and Rodriguez, I. (2012). The wiring of Grueneberg ganglion axons is dependent on neuropilin 1. *Development* 139, 2783–2791. doi: 10.1242/dev.077008
- Moine, F., Brechbuhl, J., Nenniger Tosato, M., Beaumann, M., and Broillet, M. C. (2018). Alarm pheromone and kairomone detection via bitter taste receptors in the mouse *Grueneberg ganglion*. *BMC Biol.* 16:12.
- Mori, K., Manabe, H., and Narikiyo, K. (2014). Possible functional role of olfactory subsystems in monitoring inhalation and exhalation. *Front. Neuroanat.* 8:107.
- Oelschlagel, H. A., Buhl, E. H., and Dann, J. F. (1987). Development of the nervus terminalis in mammals including toothed whales and

- humans. *Ann. N.Y. Acad. Sci.* 519, 447–464. doi: 10.1111/j.1749-6632.1987.tb36316.x
- Palaniappan, T. K., Slekienė, L., Gunhaga, L., and Patthey, C. (2019). Extensive apoptosis during the formation of the terminal nerve ganglion by olfactory placode-derived cells with distinct molecular markers. *Differentiation* 110, 8–16. doi: 10.1016/j.diff.2019.09.003
- Pfister, S., Dietrich, M. G., Sidler, C., Fritschy, J. M., Knuesel, I., and Elsaesser, R. (2012). Characterization and turnover of CD73/IP(3)R3-positive microvillar cells in the adult mouse olfactory epithelium. *Chem. Senses*. 37, 859–868. doi: 10.1093/chemse/bjs069
- Pingault, V., Bodereau, V., Baral, V., Marcos, S., Watanabe, Y., Chaoui, A., et al. (2013). Loss-of-function mutations in SOX10 cause Kallmann syndrome with deafness. *Am. J. Hum. Genet.* 92, 707–724. doi: 10.1016/j.ajhg.2013.03.024
- Pitteloud, N., Zhang, C., Pignatelli, D., Li, J. D., Raivio, T., Cole, L. W., et al. (2007). Loss-of-function mutation in the prokineticin 2 gene causes Kallmann syndrome and normosmic idiopathic hypogonadotropic hypogonadism. *Proc. Natl. Acad. Sci. U.S.A.* 104, 17447–17452. doi: 10.1073/pnas.0707173104
- Radde-Gallwitz, K., Pan, L., Gan, L., Lin, X., Segil, N., Chen, P., et al. (2004). Expression of Islet1 marks the sensory and neuronal lineages in the mammalian inner ear. *J. Comp. Neurol.* 477, 412–421. doi: 10.1002/cne.20257
- Riddiford, N., and Schlosser, G. (2016). Dissecting the pre-placodal transcriptome to reveal presumptive direct targets of Six1 and Eya1 in cranial placodes. *eLife* 5:e17666.
- Schlosser, G. (2006). Induction and specification of cranial placodes. *Dev. Biol.* 294, 303–351. doi: 10.1016/j.ydbio.2006.03.009
- Schlosser, G., Awtry, T., Brugmann, S. A., Jensen, E. D., Neilson, K., Ruan, G., et al. (2008). Eya1 and Six1 promote neurogenesis in the cranial placodes in a SoxB1-dependent fashion. *Dev. Biol.* 320, 199–214. doi: 10.1016/j.ydbio.2008.05.523
- Schmid, A., Pyrski, M., Biel, M., Leinders-Zufall, T., and Zufall, F. (2010). Gruneberg ganglion neurons are finely tuned cold sensors. *J. Neurosci.* 30, 7563–7568. doi: 10.1523/jneurosci.0608-10.2010
- Schwanzel-Fukuda, M., Garcia, M. S., Morrell, J. I., and Pfaff, D. W. (1987). Distribution of luteinizing hormone-releasing hormone in the nervus terminalis and brain of the mouse detected by immunocytochemistry. *J. Comp. Neurol.* 255, 231–244. doi: 10.1002/cne.902550207
- Schwanzel-Fukuda, M., and Pfaff, D. W. (1989). Origin of luteinizing hormone-releasing hormone neurons. *Nature* 338, 161–164. doi: 10.1038/338161a0
- Shan, Y., Saadi, H., and Wray, S. (2020). Heterogeneous origin of gonadotropin releasing hormone-1 neurons in mouse embryos detected by islet-1/2 expression. *Front. Cell. Dev. Biol.* 8:35.
- Sjodal, M., and Gunhaga, L. (2008). Expression patterns of Shh, Ptc2, Raldh3, Pitx2, Isl1, Lim3 and Pax6 in the developing chick hypophyseal placode and Rathke's pouch. *Gene Exp. Patterns* 8, 481–485. doi: 10.1016/j.gep.2008.06.007
- Sun, Y., Dykes, I. M., Liang, X., Eng, S. R., Evans, S. M., Turner, E. E., et al. (2008). A central role for Islet1 in sensory neuron development linking sensory and spinal gene regulatory programs. *Nat. Neurosci.* 11, 1283–1293. doi: 10.1038/nn.2209
- Suzuki, J., and Osumi, N. (2015). Neural crest and placode contributions to olfactory development. *Curr. Top. Dev. Biol.* 111, 351–374. doi: 10.1016/bs.ctdb.2014.11.010
- Tanaka, H., Nojima, Y., Shoji, W., Sato, M., Nakayama, R., Ohshima, T., et al. (2011). Islet1 selectively promotes peripheral axon outgrowth in Rohon-Beard primary sensory neurons. *Dev. Dyn.* 240, 9–22. doi: 10.1002/dvdy.22499
- Taroc, E. Z. M., Lin, J. M., Tulloch, A. J., Jaworski, A., and Forni, P. E. (2019). GnRH-1 neural migration from the nose to the brain is independent from Slit2, Robo3 and NELL2 signaling. *Front. Cell Neurosci.* 13:70.
- Taroc, E. Z. M., Naik, A. S., Lin, J. M., Peterson, N. B., Keefe, D. L. Jr., Genis, E., et al. (2020). Gli3 regulates vomeronasal neurogenesis, olfactory ensheathing cell formation, and GnRH-1 neuronal migration. *J. Neurosci.* 40, 311–326. doi: 10.1523/jneurosci.1977-19.2019
- Taroc, E. Z. M., Prasad, A., Lin, J. M., and Forni, P. E. (2017). The terminal nerve plays a prominent role in GnRH-1 neuronal migration independent from proper olfactory and vomeronasal connections to the olfactory bulbs. *Biol. Open* 6, 1552–1568. doi: 10.1242/bio.029074
- Thaler, J. P., Koo, S. J., Kania, A., Lettieri, K., Andrews, S., Cox, C., et al. (2004). A postmitotic role for Isl-class LIM homeodomain proteins in the assignment of visceral spinal motor neuron identity. *Neuron* 41, 337–350. doi: 10.1016/s0896-6273(04)00011-x
- Thor, S., Ericson, J., Brannstrom, T., and Edlund, T. (1991). The homeodomain LIM protein Isl-1 is expressed in subsets of neurons and endocrine cells in the adult rat. *Neuron* 7, 881–889. doi: 10.1016/0896-6273(91)90334-v
- Vanacker, C., Trova, S., Shruti, S., Casoni, F., Messina, A., Croizier, S., et al. (2020). Neupilin-1 expression in GnRH neurons regulates prepubertal weight gain and sexual attraction. *EMBO J.* 39:e104633.
- Wang, F., Zhao, S., Xie, Y., Yang, W., and Mo, Z. (2018). De novo SOX10 nonsense mutation in a patient with kallmann syndrome, deafness, iris hypopigmentation, and hyperthyroidism. *Ann. Clin. Lab. Sci.* 48, 248–252.
- Wirsig-Wiechmann, C. R. (2004). Introduction to the anatomy and function of the nervus terminalis. *Microsc. Res. Tech.* 65:1. doi: 10.1002/jemt.20115
- Wray, S., Grant, P., and Gainer, H. (1989). Evidence that cells expressing luteinizing hormone-releasing hormone mRNA in the mouse are derived from progenitor cells in the olfactory placode. *Proc. Natl. Acad. Sci. U.S.A.* 86, 8132–8136. doi: 10.1073/pnas.86.20.8132
- Yang, L., Cai, C. L., Lin, L., Qyang, Y., Chung, C., Monteiro, R. M., et al. (2006). Isl1Cre reveals a common Bmp pathway in heart and limb development. *Development* 133, 1575–1585. doi: 10.1242/dev.02322
- Yin, W., and Gore, A. C. (2006). Neuroendocrine control of reproductive aging: roles of GnRH neurons. *Reproduction* 131, 403–414. doi: 10.1530/rep.1.00617
- Yoon, H., Enquist, L. W., and Dulac, C. (2005). Olfactory inputs to hypothalamic neurons controlling reproduction and fertility. *Cell* 123, 669–682. doi: 10.1016/j.cell.2005.08.039
- Zhang, G., Li, J., Purkayastha, S., Tang, Y., Zhang, H., Yin, Y., et al. (2013). Hypothalamic programming of systemic ageing involving IKK-beta, NF-kappaB and GnRH. *Nature* 497, 211–216. doi: 10.1038/nature12143
- Zhou, X., Li, W. W., Wu, Q. Y., Yu, M. M., and Xia, X. Y. (2017). [Kallmann syndrome with deafness caused by SOX10 mutation: advances in research]. *Zhonghua Nan Ke Xue* 23, 838–841.
- Zhuang, S., Zhang, Q., Zhuang, T., Evans, S. M., Liang, X., Sun, Y., et al. (2013). Expression of Isl1 during mouse development. *Gene Exp. Patterns* 13, 407–412. doi: 10.1016/j.gep.2013.07.001
- Zou, D., Silvius, D., Fritsch, B., and Xu, P. X. (2004). Eya1 and Six1 are essential for early steps of sensory neurogenesis in mammalian cranial placodes. *Development* 131, 5561–5572. doi: 10.1242/dev.01437

Conflict of Interest: The authors declare that the research was conducted in the absence of any commercial or financial relationships that could be construed as a potential conflict of interest.

Copyright © 2020 Taroc, Katreddi and Forni. This is an open-access article distributed under the terms of the Creative Commons Attribution License (CC BY). The use, distribution or reproduction in other forums is permitted, provided the original author(s) and the copyright owner(s) are credited and that the original publication in this journal is cited, in accordance with accepted academic practice. No use, distribution or reproduction is permitted which does not comply with these terms.